The crystal structure of augmenter of liver regeneration: A mammalian FAD-dependent sulfhydryl oxidase

CHIA-KUEI WU,[1,2] TAMARA A. DAILEY,[1] HARRY A. DAILEY,[1] BI-CHENG WANG,[1] AND JOHN P. ROSE[1]

[1]Department of Biochemistry and Molecular Biology, University of Georgia, Athens, Georgia 30602, USA
[2]HIV Drug Resistance Program, National Cancer Institute, Frederick, Maryland 21702–1201, USA

(RECEIVED October 30, 2002; FINAL REVISION January 27, 2003; ACCEPTED February 3, 2003)

Abstract

The crystal structure of recombinant rat augmenter of liver regeneration (ALRp) has been determined to 1.8 Å. The protein is a homodimer, stabilized by extensive noncovalent interactions and a network of hydrogen bonds, and possesses a noncovalently bound FAD in a motif previously found only in the related protein ERV2p. ALRp functions in vitro as a disulfide oxidase using dithiothreitol as reductant. Reduction of the flavin by DTT occurs under aerobic conditions resulting in a spectrum characteristic of a neutral semiquinone. This semiquinone is stable and is only fully reduced by addition of dithionite. Mutation of either of two cysteine residues that are located adjacent to the FAD results in inactivation of the oxidase activity. A comparison of ALRp with ERV2p is made that reveals a number of significant structural differences, which are related to the in vivo functions of these two proteins. Possible physiological roles of ALR are examined and a hypothesis that it may serve multiple roles is proposed.

Keywords: FAD dependent sulfhydryl oxidase; augmenter of liver regeneration; crystal structure; ERV2

Augmenter of liver regeneration (ALR) and its yeast homologs essential for respiration and viability1 (ERV1) and ERV2 are representatives of a eukaryotic family of sulfhydryl oxidases, which are capable of catalyzing disulfide bond formation for a number of proteins. Of the ALR/ERV proteins that have been characterized, all contain a conserved C-X-X-C motif, which is distinct from that found in thioredoxin and glutaredoxin reductases, and a noncovalently bound flavin adenine dinucleotide (FAD). ALRp is a homodimeric mammalian protein with remarkable thermostability and resistance to denaturants and requires harsh conditions to release the FAD.

Experimental evidence has been presented to suggest that ALRp serves as a hepatotrophic growth factor during liver regeneration (Hagiya et al. 1994) and as a generalized growth factor during pancreas transplant/regeneration (Adams et al. 1998). The role of the ALR yeast homologs ERV1p and ERV2p obviously cannot be in tissue regeneration. The yeast ERV2p and its counterpart protein disulfide isomerase (PDI) have been proposed to function in the endoplasmic reticulum in protein disulfide bond formation (Sevier et al. 2001). For ERV1 the most recent data from genetic studies support a role for ERV1p in transport/maturation of Fe/S clusters in the cytoplasm of yeast (Lange et al. 2001). There exist a number of additional ALR/ERV homologs in nature. Some double-stranded DNA viral proteins, such as E10R of vaccinia virus, contain the ALR/ERV1 motif and these have been shown to be active in a redox-mediated maturation of viral particles (Senkevich et al. 2000). These reports suggest that the ALR/ERV family members participate in a wide variety of essential intra- and extracellular reactions.

The ALR/ERV1 motif has also been found in a number of recently identified eukaryotic oxidoreductases typified by

Reprint requests to: John P. Rose, Department of Biochemistry and Molecular Biology, B204B Life Sciences Building, University of Georgia, Athens, GA 30602, USA; e-mail: rose@BCL4.bmb.uga.edu; fax: (706) 542-3077.

Article and publication are at http://www.proteinscience.org/cgi/doi/10.1110/ps.0238103.

egg white sulfhydryl oxidase (Hoober et al. 1999). These proteins, which possess both an ALR/ERV1 and thioredoxin-like motif, have been shown to catalyze sulfhydryl oxidase reactions for a wide range of protein substrates in what may best be described as a chaperone function. Additional proteins possessing an ALR/ERV1 motif are the human and chicken Q6 inhibitors of cell growth, which function in the reversible silencing of the division of fibroblasts (Coppock et al. 1998), and SOx-3, which is suggested to be involved in cell cycle regulation (Musard et al. 2001).

Below we present the structure of recombinant rat ALR at 1.8 Å resolution and demonstrate that the rigidity, dimer structure, and extreme stability of ALRp are attributable to an unusual network of salt bridges that are only present in ALRs but not ERV1/ERV2 proteins. The FAD-binding motif for ALR, first described by Rose et al. (1999), is similar to that recently found in ERV2p (Gross et al. 2002) and is unique because of the spatial orientation of the FAD and the presence of a series of stacked aromatic ring side chains. In addition to the structural data, experimental data are presented to identify the disulfide involved in flavin redox cycling and to show that the protein's FAD undergoes conversion to a stable semiquinone rather than a completely reduced flavin in the presence of dithiothreitol. Complete reduction of the protein in vitro requires the addition of dithionite.

Results

General features

ALRp is a cone-shaped helical bundle (α1–α5) with dimensions of ~32 × 26 × 20 Å similar to the recently reported Erv2p (Gross et al. 2002). A bound FAD molecule sits at the mouth of the cone. ALRp is a 30-kD homodimer (Fig. 1A) linked head-to-tail by two (C15–C124′ and C15′–C124) intermolecular disulfide bonds (here ′ denotes an adjacent molecule). There are four ALRp molecules (two dimers) in the crystallographic asymmetric unit. The refined model presented here consists of residues 14–124 of each monomer, one FAD molecule bound to each monomer, and 310 solvent molecules modeled as water.

Residues 1–13 and 125 of the enzyme were not observed in the electron density maps and are presumed to be disordered. The observed polypeptide chain begins at residue 14 located at the mouth of the cone and begins a short loop ending at α1 (residues 18–36), a 27-Å long helix. A β-turn (residues 38–41) forms the tip of the cone. Helix α2 (residues 42–60) running antiparallel to α1, returns the chain back to the mouth of the cone and is followed by a short loop ending at helix α3 (residues 62–76) that contains residues C62 and C65 (observed as a right-handed hook disulfide), the putative catalytic site. The catalytic disulfide is preceded by Pro 61, a highly conserved *cis* proline (Fetrow et al. 1999), forming a P-C-X-X-C motif common to the glutaredoxin/thioredoxin family. After α3, the chain loops back to the bottom of the cone and enters helix α4 (residues 82–101), a 28.5-Å helix that represents the most conserved region in ALR/ERV1 proteins. Helix α4 then brings the chain back to the mouth of the cone where it loops back and enters helix α5 (residues 107–116). After α5 the chain forms an extended loop from the cone surface ending at C124, the last visible carboxy-terminal residue.

The spatial orientation of the FAD molecule places the flavin moiety in the mouth of the cone packed against helices α1, α2, and α3. The adenine moiety of FAD loops between α1 and α4 and packs against helices α4 and α5. Specific interactions between FAD and ALR are mostly located at the AMP moiety that forms several hydrogen bonds with helices α4 and α5 and plays a crucial role in the protein–ligand recognition.

Other stabilizing interactions

The six ALRp cysteine residues all participate in disulfide bridge formation. The terminal cysteines C15 and C124, as mentioned previously, form two head-to-toe intermolecular disulfide bonds. This pair of disulfides is accommodated by the presence of a 14-Å amino-terminal loop, which extends from one molecule toward the carboxyl -terminus of the other ALR molecule. In addition, two intramolecular disulfide bridges (C62–C65 and C91–C108) are observed and are located on opposite sides of the FAD ligand. The C62–C65 pair is located 3.5 Å from N5 of the isoalloxazine ring of the FAD ligand and forms the putative catalytic site. The C91–C108 disulfide also contacts the FAD ligand where the oxygen of C91 forms a hydrogen bond with AN6 of the adenine moiety.

Forty-four of the 125 ALRp residues (35%) possess charged side chains with a net charge of −2 for the protein. Of the nine salt bridges observed in ALRp more than 50% (R75–E96, E96–R72, R72–D68, and D68–K100) are involved in an extensive network (Fig. 2), a rather unusual feature in a small protein. In addition, an intermolecular salt bridge, K58–D48′, is located on the dimer surface. The abundance of disulfide and salt bridges make the ALRp molecule a rigid structure and probably accounts for ALRp's thermostability and resistance to some denaturants as described in the Materials and Methods section.

Dimer interface

Most of the hydrophobic residues in ALRp are located in the interface between helices α1 and α2 and form an extended hydrophobic patch that is involved in dimerization. The dimer interface occupies ~720 $Å^2$ (~24.6% of the total surface area) of the monomer surface (Fig. 3). The subunits in the dimer are related by a pseudo twofold symmetry axis

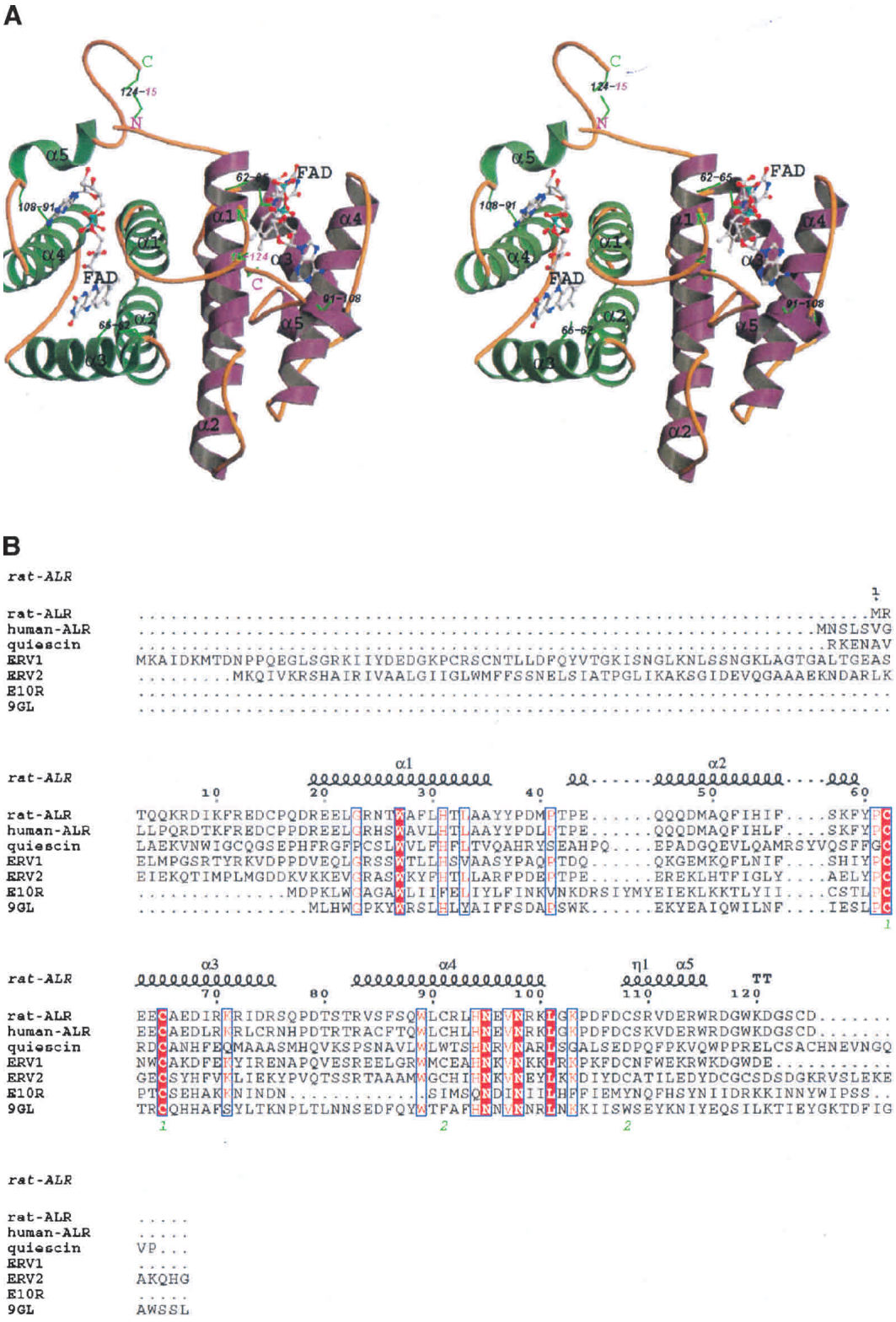

Figure 1. (*A*) A stereo view of ALR homodimer showing its FAD ligand. The ALRp monomer (32 × 26 × 20 Å), is cone-shaped with the FAD isoalloxazine moiety sitting in the mouth of the cone, forming the novel helix-bundle FAD-binding motif unique to the ALR/ERV protein family. The dimer is stabilized in part by two intersubunit disulfide bonds, not observed in ERV2p, that are formed between the amino- and carboxy-terminal cysteines from each molecule that link the monomers in a head-to-tail fashion. (*B*) Sequence and structure alignment among the ALR/ERV family proteins, including rat-ALRp (BAA06399), human-ALRp (XP_034465), ALR domain of rat quiescin Q6 (AAG53892), ERV1p (NP_011543), ERV2p (NP_015362), E10R (NP_048164), and 9GL (NP_042767). Most of the conserved sequences shown related to FAD binding.

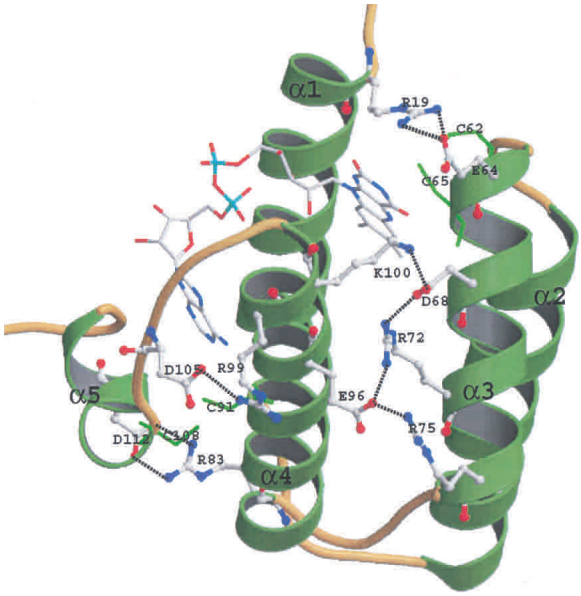

Figure 2. A view of the extensive salt bridge network found in the ALRp structure. The monomer's nine salt bridge pairs include D117–R116, D113–R110, D112–R83, D105–R99, E96–R72, R75–E96, R72–D68, D68–K100, and E64–R19 (D117–R116 and D113–R110 are not shown in this figure). Among these, E64–R19, R75–E96, E96–R72, R72–D68, and D68–K100 form a network that bridges helices α3 and α4, whereas the other four form a network that links helices α4 and α5.

with the FAD-binding motifs present on a common face. The major dimeric interactions are located on helices α1 and α2 and are distant from the FAD-binding region. Residues P16, F52, F56, F59, and P61 form a network of hydrophobic interactions. In addition, four hydrogen bonds and two salt bridges are also found at the dimer interface (Fig. 4). The interfacial disulfides, however, are not conserved among the ALR/ERV family and are not required for dimerization as evidenced by the ERV2p structure that lacks the amino-terminal cysteine and by fact that site directed mutagenesis of C124 to S124 in ALRp does not disrupt dimer formation as determined by SDS gel electroporesis with and without reductant. The fact that the intersubunit disulfide is not needed for ALRp dimerization is interesting and may indicate that this disulfide is an artifact, as both the mature ALR and ERV1 proteins, but not ERV2p, contain an additional C-X-X-C motif at the amino terminus.

ALR–FAD interaction

In general the catalytic function of the FAD is attributable to the isoalloxazine ring, with the ribityl phosphate and the AMP moieties serving to stabilize cofactor binding to the protein. Although the FAD serves a role in two electron redox reactions, it is the surrounding protein environment and FAD orientation that specifies many of the catalytic properties of the flavin ring and the redox potential (Mathews 1991). In ALRp the noncovalently bound FAD is present in an extended form with an unusual directionality in the adenine moiety (Fig. 5; Dym and Eisenberg 2001). The conformation is stabilized in part by two internal hydrogen bonds within the FAD (AO2–O5* and O3*–AO1). The orientation of the AMP tail places the adenine and isoalloxazine rings in an approximately parallel orientation (Fig. 6). The protein region between the adenine and isoalloxazine moieties is occupied by the side chains of the conserved residues H94 and W27, which are also stacked parallel to the FAD ring structures. The isoalloxazine ring and the adenine ring sandwich the side chains of W27, H31, and H94 with a spacing of 3.6 ± 0.1 Å between each pair. The net result is a unique stacked ring structure that is additionally capped at each end by Y60 and F106. This ring substructure is also shared by ERV2p and is a conserved feature for ALR/ERV family proteins.

ALR has a FAD-binding motif that uses a five-helix bundle. In ALRp, helices α1, α2, and α3 interact with the flavin moiety through a number of hydrophobic interactions

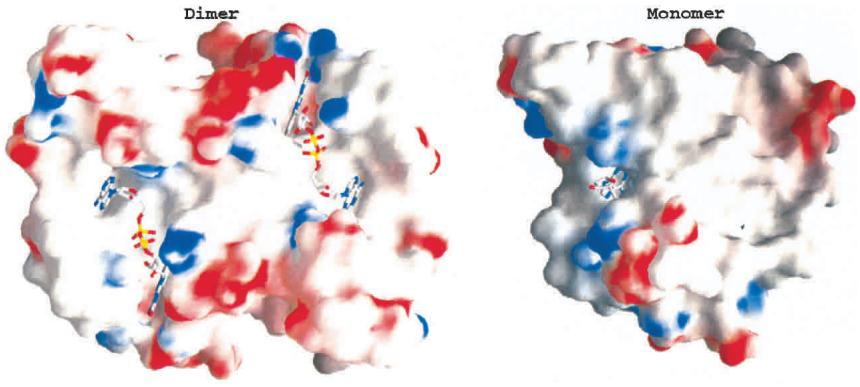

Figure 3. A surface representation of the ALRp monomer and dimer. The hydrophobic area (in white) of the monomer is mostly buried in the dimer configuration and is largely responsible for the dimerization.

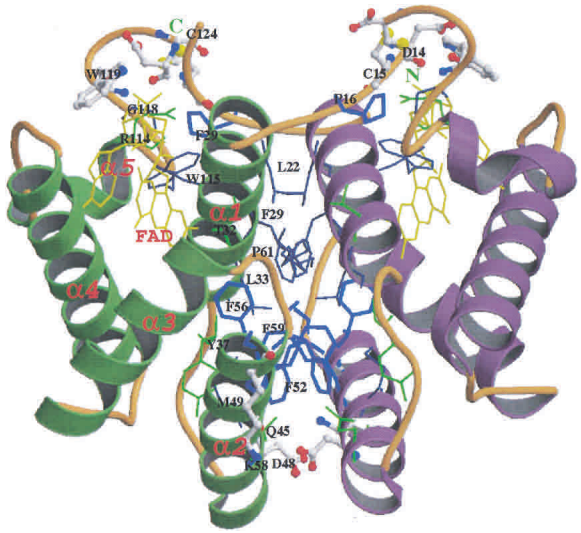

Figure 4. The detailed dimer interactions including nonbonded (in lines) and bonded interactions (in ball-and-stick formation). There are 20 contacting residues on the dimer interface (P16, Q17, L22, N25, A28, F29, T32, L33, Y37, Gln45, M49, Gln51, F52, I55, F59, F56, P61, W115, R116, G118) contributing to hydrophobic interactions. The bonded interactions include four hydrogen bonds (W119–D14′, R114–C15′), two salt bridges (K58–D48′), and two disulfide bonds (C15–C124′).

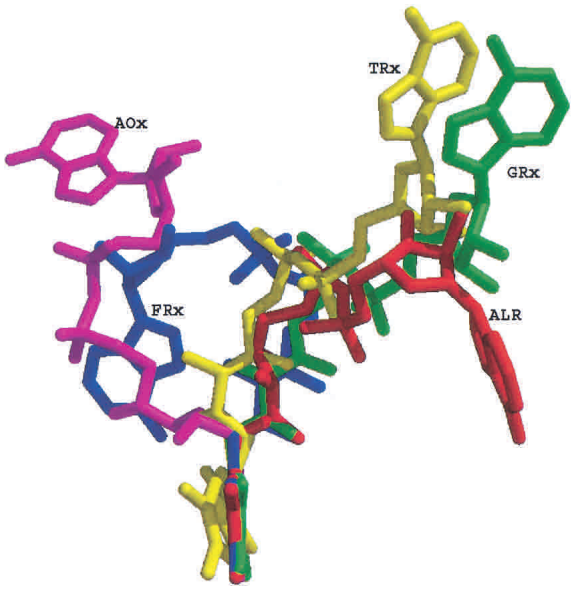

Figure 5. The superposition of conformations of FAD from various representative FAD-containing proteins based on isoalloxazine ring. The extended conformations are represented by glutathione reductase (GRx) in green (PDB code 1ger), thioredoxin reductase (TRx) in yellow (1cl0), alcohol oxidase (AOx) in magenta (1e8g), and the bent form is from ferrodoxin reductase (FRx) in blue (1a8p). FAD in ALRp (red) has a special adenine moiety directionality that folds back in approximately parallel to its isoalloxazine ring.

with the isoalloxazine ring and two hydrogen bonds (O2–W27, NE2), and (O1P–K103, NZ) to the FAD backbone. Helices α4 and α5 interact with the AMP moiety mainly through hydrogen bonds: (AN3–W115, NE), (AN6–C91, O), (AN7–N98, ND2), (AO2–H94, NE2), and (AO2*–R114, NE). These interactions (Fig. 7) include many of the most conserved residues in the ALR/ERV family and feature the recognition of FAD by ALR/ERV1 proteins. In addition, conserved residues W27, H31, C62, C65, H94, N95, V97, N98, and L101 surround the binding pocket.

Differences between ALRp and ERV2p

The structure of the yeast ALR analog ERV2p has recently been published (Gross et al. 2002). The two structures, as one might expect, are very similar and can be superimposed (Fig. 8) with an r.m.s.d. of 0.64 Å (main chain) for the helical core (ALRp residues 19–111 and ERV2p residues 78–170). The relationship of the monomers making up the dimer in these two enzymes is slightly different and may be attributable to the presence of the ALRp intersubunit disulfide bridges that are not present in ERV2p or the C-X-C C terminal motif present in ERV2p, which is not present in ALRp. The variations in both the amino and carboxyl termini may also account for the differences in the observed redox pathway and possibly different specificities in protein substrates.

Another difference found is the abundance of salt bridges in ALRp that are not present in the ERV2 protein. The

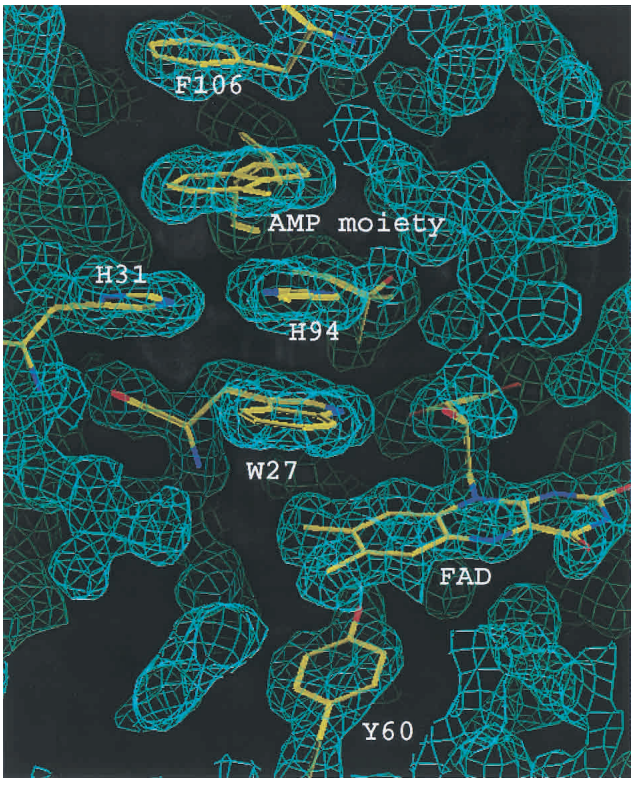

Figure 6. The electron density (2Fo–Fc) map in the ring-stacking region of ALRp consists of FAD and residues W27, H31, H94, Y60, and F106.

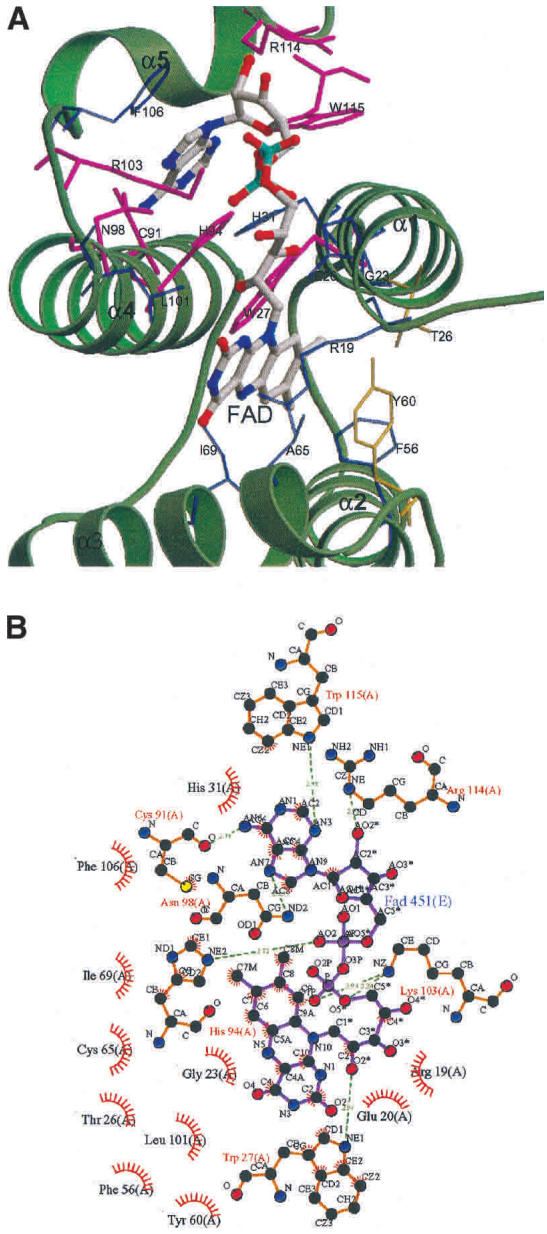

Figure 7. (*A*) A MOLSCRIPT representation of the ALRp FAD-binding site showing the location of FAD in the mouth of the cone formed by helices α1, α2, and α4. (*B*) A LIGPLOT representation of the ALRp FAD-binding site. The residues in magenta are involved in hydrogen bonding with FAD, and residues in blue have hydrophobic interactions with FAD. These involved residues are also the most conserved residues in ALR/ERV protein family.

interfacial salt bridges (D58–K48′ and D58′–K48), however, are in common and become a conserved dimer-stabilizing interaction in ALR/ERV family of proteins.

Mechanism

ALRp is readily reduced by DTT, but not by 2-mercaptoethanol or glutathione. In the presence of excess DTT, the oxidized flavin is reduced to a neutral semiquinone (Fig. 9). In the absence of added oxygen this spectrum does not change and the semiquinone is only reduced by the addition of dithionite. Previously in egg white sulfhydryl oxidase a 570-nm feature was described that appeared during flavin reduction. This feature was ascribed to a flavin–thiolate charge transfer complex between the FAD and the thioredoxin-like C-X-X-C residues (Hoober and Thorpe 1999). It should be noted that this complex involves a partially reduced FAD and is proposed to be a two-electron reduction intermediate (EH_2) that occurs before full flavin and disul-

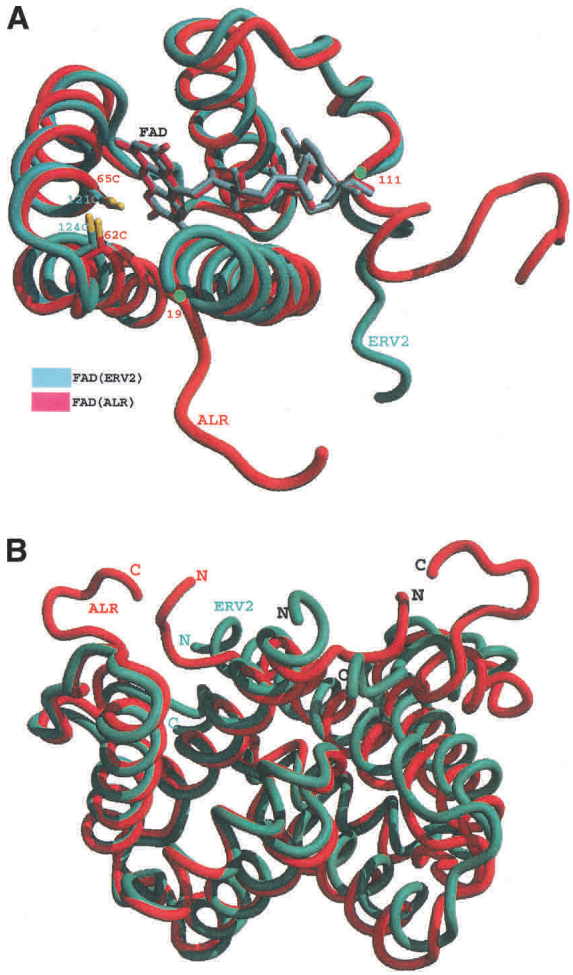

Figure 8. (*A*) The superposition of the ALRp (red) and ERV2p, PDB entry 1JR8 (cyan) monomers. The main chain r.m.s.d. for the conserved core (ALRp residues 19–111 and ERV2p residues 78–170) is 0.64 Å. The spatial relation of FAD and catalytic cysteines in the two structures are also very similar. It is plausible that the core structure for the protein family is conserved yet the individual enzymatic function varies according to the terminal regions. (*B*) The superposition of the ALRp and ERV2p dimers using the same color scheme. Although the ERV2p dimer is a slightly more open structure, the major structural differences observed between the two structures are at the amino and carboxyl termini. This is because in ALRp the amino and carboxyl termini are linked by an intersubunit disulfide bridge not present in ERV2p, as it lacks the amino-terminal cysteine.

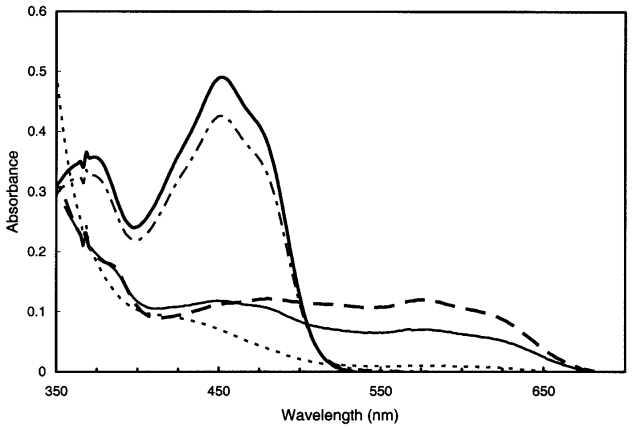

Figure 9. Reduction of ALRp by DTT. The visible spectra of recombinant rat ALRp in 20 mM sodium phosphate buffer at pH 7.0 is shown in the top (solid line) scan. The spectra at 30 (— ● —), 60 (— —), and 90 (- - -) sec after the addition of 1 mM DTT are shown as the absorbance at 450 nm decreases. The spectrum obtained at 90 sec persists for at least 10 min and is not altered by the addition of more DTT. The final spectrum (● ● ●) is that of ALRp reduced by dithionite.

fide reduction. In ALR there is no evidence for such a complex. Unlike egg white sulfhydryl oxidase, ALRp does not contain the distinct thioredoxin motif and its associated cysteines. However, it does possess a disulfide (C62 and C65) adjacent to the flavin ring of its FAD. Due to the proximity of these cysteine residues to the FAD, it may be anticipated that they might play a role in FAD reduction by DTT. Mutagenesis of either one of these cysteine residues to a serine (e.g., C62S and C65S), results in a molecule with stoichiometric amounts of bound FAD, which is not reduced by DTT. This observation supports a role for these two residues in redox cycling of the FAD moiety.

Discussion

We have detailed the structure of recombinant rat ALRp at 1.8 Å resolution. The structure reveals a unique FAD-binding motif, a region containing side chain rings in a stacked, parallel orientation as has recently been reported in ERV2p, and an extensive salt bridge network that is unique to ALR. A number of proteins are now known to possess both an ALR motif and a separate thioredoxin motif. Among these proteins, the best characterized is egg white sulfhydryl oxidase whose FAD is reduced by DTT, glutathione, and 2-mercaptoethanol (Hoober et al. 1999). Total reduction of this FAD requires four electrons per molecule. The proposed reaction involves an intermediate thiolate-to-flavin charge transfer complex with complete and stable reduction of the FAD occurring only after reduction of the thioredoxin-like disulfide (Hoober and Thorpe 1999).

In ALRp, which lacks the separate thioredoxin-like domain, only partial FAD reduction occurs with DTT. This reaction clearly involves the disulfide at C62 and C65, as mutagenesis of either of these residues to serine results in an ALRp whose FAD cannot be reduced by DTT. Interestingly, in the presence of excess DTT as reducing agent and the absence of oxygen one sees only the formation of a semiquinone and not a completely reduced flavin. Why this occurs is not clear, but this does distinguish ALRp from ERV2p, which has been reported to be completely reduced by DTT (Gross et al. 2002).

Several suggestions for a function of ALR/ERV1 proteins have been forwarded and can be imagined due to the presence of the sulfhydryl oxidase activity. It is now clear that intracellular redox status is central to the control of a variety of cellular functions including proliferation and apoptosis. Proteins such as thioredoxin, which plays a central role in the redox status of glutathione, and peroxiredoxins, have gathered increased attention for their roles as regulators of cellular functions. If ALR does play a role in redox status, then the corresponding redox couple molecule remains to be identified. There is substantial evidence that an ALR/ERV1 homolog (E10R) can oxidize viral glutaredoxin (G4L) in protein disulfide bond formation during viral coat maturation (Senkevich et al. 2002; White et al. 2002), but to date no data exist to suggest that this is the role of ALR or ERV1 in cells.

Before the present work, it was known that exogeneously administered serum ALR, through some unknown means, affected the rate of mammalian liver regeneration (Gandhi et al. 1999), but that ALR was found intracellularly in essentially all cell types. In fact, ALR was originally isolated as a factor that augmented the rate of liver regeneration when injected into animals with a regenerating liver. One possible manner in which ALR may function in liver regeneration may now be hypothesized. Circulating ALR, released as a consequence of liver damage, might interact with surface receptors of G protein-coupled receptors or protein–tyrosine kinase receptors (RPK) on NK cells (Lu et al. 2002). It could be envisioned that the sulfhydryl oxidase activity of ALR might catalyze the cross-linking of two monomers of RPK to form an active signaling complex, or with G protein receptors, a receptor disulfide switch may be oxidized to turn on or off a response. In either of these cases, this interaction would signal a cellular response resulting in the observed growth stimulatory features reported for ALR. This would not, however, explain the role of ERV1 in yeast and by analogy the intracellular role of ALR in healthy cells.

A recent report presents interesting genetic data from yeast that are consistent with a role for ERV1 (and by inference ALR) in transport of iron sulfur clusters from the mitochondrion to cellular proteins that possess [4Fe–4S] clusters (Lange et al. 2001). Although this proposal is of great interest, the current structure does not make clear how such a function may be mediated. Assuming that the cluster

ligands are cysteines, there needs to be four such side chains within a spatial distance that would allow coordination. The only obvious cysteine pairs are C62–C65 and C91–C108. Although these are both located within the FAD-binding cone, they appear to be spatially too distant from each other to simultaneously coordinate a [4Fe–4S] cluster without significant molecular movement. Although it could be envisioned that the extensive hydrogen-bonding network may function in a concerted molecular rearrangement resulting in a cluster transporter, additional studies will be required to investigate this possibility. Another hypothesis may be considered with regard to this model, in which ALR/ERV1 may serve a chaperone function in conjunction with another [4Fe–4S]-carrying protein. This second protein may "replace" the thioredoxin-containing motif found in the sulfhydryl oxidase family of proteins with another accessory protein that gives the complex its cluster exchange capability. Evaluation of this possibility should be experimentally possible in yeast by using a two-protein hybrid system.

Recently the structure of ERV2p was presented with data showing that it is a disulfide oxidase in the endoplasmic reticulum (Sevier et al. 2001). Interestingly, it was proposed that a C-X-C motif near the carboxyl terminus was involved in the oxidase activity based on the structure of one molecule in the crystallographic asymmetric unit. If this proposed motif is truly essential for oxidase activity in ERV2p, then ALRp and ERV1p must carry out their oxidase activities in a different fashion, as these two proteins lack this motif. It may be that ERV2p requires this flexible C-X-C motif to allow it to interact at a distance with a variety of ER substrates, whereas ALR/ERV1 may both be more specific and restricted with regard to their redox pair in the cytoplasm/mitochondrion. This would certainly be the case if ALR/ERV1 functions in iron–sulfur cluster translocation as previously suggested.

A second interesting finding with ERV2p in contrast to ALRp is the need for disulfide bond formation between cys 121 and either cys 176 or 178 to stabilize the dimeric structure of ERV2p. ALRp forms a stable dimer in the absence of this bond and remains as a dimer in the presence of reducing agents. This is attributable to the strong noncovalent interactions between the two monomers of ALRp, which are missing in ERV2p. One point to consider is that ERV2p is a proteolytic truncation of ERV2 and is missing the putative ER membrane attachment region. It is probable that the holoprotein of ERV2p is stabilized as a dimer by this membrane attachment motif as it is difficult to see how ERV2p could function in vivo without such dimer stabilization.

In summary, the ALR/ERV FAD C-X-X-C motif is widely found in nature and appears to participate in a variety of biological functions. The comparison of ALRp with ERV2p demonstrates that conservation of a functional oxidase activity with a unique fold can be accomplished with little sequence conservation outside of the essential motifs and that even a necessary dimerization is accomplished in distinct fashions. In addition, it appears that there exist significant bodies of data to indicate that ALR has functions both inside cells and outside of select cell types. Such a dual function for a protein is certainly not unique. Cytochrome c is an excellent example of a protein that has two distinct roles in the cell and one could imagine that ALR may have evolved two distinct roles in higher animals. It will be of interest to determine whether a homolog of ERV2 also exists in animal cells and whether ERV2p has similar cell proliferation stimulatory features as has been reported for ALR.

Materials and methods

Protein expression and purification

For this study, the 125-residue ALR carboxy-terminal fragment (ALRp) corresponding to the physiologically active protein originally isolated by Francavilla et al. (1987) from regenerating liver was cloned into a pTF20 expression vector containing Tac promoter. The mature ALR protein contains an additional 73 amino-terminal leader sequence similar to that observed in the mature ERV1 protein (Lisowsky 1996). Protein was expressed in *Escherichia coli* strain BC21 with added 10 μM riboflavin in the culture media. The cell pellet was resuspended in the buffer containing 30 mM Tris at pH 8.0, 200 mM NaCl, and 0.1 mM PMSF (phenylmethylsulphonyl fluoride), sonicated, and then centrifuged for 20 min at 10,000*g*. The resulting supernatant was then incubated at 65°C for 30 min. Precipitated protein was removed by centrifugation (20 min at 10,000*g*) and the soluble protein fraction mixed with 6 volumes of ethanol, stirred for 2 h at 4°C, and centrifuged. The resulting pellet was suspended in 150 mM ammonium acetate at pH 6.0, filtered, and concentrated to 10 mg/mL. Further purification used chromatography on a Mono Q 5/5 column followed by gel filtration on a Superdex 16/60 column (Pharmacia).

Mutagenesis

Site-directed mutagenesis to create C62S, C65S, the double mutant C62S/C65S, and C124S of ALRp were accomplished using Quikchange mutagenesis (Stratagene).

UV-visible spectra of the protein were obtained using a Cary 1G spectrophotometer. Details are in the Figure 9 legend.

Crystallization

Initial crystallization of human ALR was unsuccessful due to poor solubility of the protein. Rat ALRp, which has 92% sequence identity with human ALRp, is soluble at concentrations sufficient to set up crystallization experiments. Crystallization protocols have been described previously for the native protein (Rose et al. 1997), yielding orthorhombic crystals with unit cells of a = 108.2 Å, b = 125.1 Å, and c = 38.5 Å. The heavy atom derivative search encountered nonisomorphism in which the a-axis in derivatives varied from 101 Å to 109 Å. Se-Met rALR was, therefore, prepared (Doublie 1997) and crystals of Se-Met rALR were obtained by the microseeding with native crystals.

Table 1. *Statistics from the crystallographic analysis*

Crystal									
Space group:	$P2_12_12$								
a	106.99								
b	123.13								
c	37.93								
MAD analysis									
Beamline:	NSLS X12C, Small Brandeis CCD								
Number of Crystals:	1								
Phi step:	0.5 degrees								
2θ:	0.0								
Total Rotation:	480 degrees [120° + (120° inverse beam), collected twice]								
Data processing:	HKL 1.9.1								
Wavelength (Å)	Resolution (Å)	Completeness*	Redundancy	R_{sym} (%)*					
λ_1: 0.9787	40–2.20	92.5 (55.2)	13.3	5.3 (7.1)					
λ_2: 0.9790	40–2.20	92.7 (56.4)	14.4	5.2 (7.2)					
λ_3: 0.9500	40–2.20	95.6 (66.5)	14.4	5.6 (7.7)					
*outer shell 2.24–2.2 Å values in parentheses									
Phasing statistics (2.4 Å)									
Dmin (Å)	TOTAL	8.22	5.33	4.21	3.59	3.18	2.88	2.66	2.48
Mean Figure of Merit:	0.71	0.71	0.79	0.78	0.74	0.75	0.74	0.67	0.56
Refinement data									
Beamline:	APS 17ID (IMCA-CAT), Bruker 2X2 mosiac CCD								
Number of Crystals:	1								
Phi step:	0.25 degrees								
2θ:	0.0								
Total Rotation:	140 degrees (four 35 degree data runs)								
Data processing:	SMART/SAINT								
Wavelength (Å)	Resolution (Å)	Completeness*	Redundancy	R_{sym} (%)*					
λ_1: 0.9790	99–1.6	76.5 (40.5)	4.8	7.8 (17.3)					
*outer shell 1.7–1.6 Å values in parentheses									
Refinement									
Program:	CNS 1.0	r.m.s.d. from ideality							
Resolution (Å):	27.65–1.80	Bond lengths:	0.006Å						
Completeness (%):	88.1	Bond angles:	1.5°						
Rcryst	0.202/0.211	Dihedral angles:	18.0°						
Rfree	0.240/0.268	Improper angles:	1.32°						

Data collection, structure determination, and refinement

Phasing data were collected under standard cryogenic conditions by a three-wavelength multiwavelength anomalous dispersion (MAD) experiment carried out at the National Synchrotron Light Source (Beamline X12C) Brookhaven National Laboratory at X-ray wavelengths corresponding to the peak (λ_1), and inflection point (λ_2) of the selenium absorption edge, plus a high energy (λ_3) remote point. The experiment was then repeated to double the redundancy of the data sets. Data were recorded on the small Brandeis CCD detector and indexed, integrated, and scaled using HKL 1.91 (Otwinowski and Minor 1997). The high resolution data for refinement were collected under cryogenic conditions on a Bruker 2X2 Mosiac CCD detector at the Advanced Photon Source (Beamline ID-17 IMCA-CAT), Argonne National Laboratory and processed with the Bruker SMART/SAINT software. Details of the data collection and processing for all four data sets are given in Table 1.

Solve v1.0 (Terwilliger and Berendzen 1999) was used to determine the eight selenium atom positions in the asymmetric unit and the initial protein phases. Using the selenium positions and bones points as guides in O (Jones 1991), 440 residues, 88% of the total structure could be readily fit into the experimental electron density map.

The structure was refined using CNS v1.0 (Brunger et al. 1998) against data in the range from 27.65 to 1.8 Å resolution (88.1% complete), and converged after simulated annealing and solvent addition (Perrakis et al. 1999) to give an R value of 0.205 and an R_{free} value of 0.245. The final model consisted of residues 14–125 for each four molecules in the asymmetric unit, four FAD molecules and 620 solvent atoms treated as water. Residues 1–13 and 125 are presumably disordered. Details of the refinement are collected in Table 1. The coordinates have been deposited in the Protein Data Bank, entry 1OQC.

Acknowledgments

This work was supported in part by finds from the University of Georgia Foundation and Georgia Research Alliance, and a generous gift of beam time from Art Robbins Bayer Corp. Data for this study were measured at beamline X12C of the National Synchrotron Light Source (NSLS) and 17-ID (IMCA-CAT) Advanced Photon Source (APS). Financial support for these facilities comes from (X12C, NSLS) the National Center for Research Resources

of the National Institutes of Health; U.S. Department of Energy, Basic Energy Sciences, Offices of Biological and Environmental Research; (IMCA-CAT) the companies of the Industrial Macromolecular Crystallography Association; and (APS) U. S. Department of Energy, Basic Energy Sciences, Office of Science, under Contract No. W-31–109-Eng-38.

The publication costs of this article were defrayed in part by payment of page charges. This article must therefore be hereby marked "advertisement" in accordance with 18 USC section 1734 solely to indicate this fact.

References

Adams, G.A., Maestri, M., Squiers, E.C., Alfrey, E.J., Starzl, T.E., and Dafoe, D.C. 1998. Augmenter of liver regeneration enhances the success rate of fetal pancreas transplantation in rodents. *Transplantation* **65:** 32–36.

Brunger, A.T., Adams, P.D., Clore, G.M., DeLano, W.L., Gros, P., Grosse-Kunstleve, R.W., Jiang, J.S., Kuszewski, J., Nilges, M., Pannu, N.S., et al. 1998. Crystallography & NMR system: A new software suite for macromolecular structure determination. *Acta Crystallogr. D Biol. Crystallogr.* **54:** 905–921.

Coppock, D.L., Cina-Poppe, D., and Gilleran, S. 1998. The quiescin Q6 gene (QSCN6) is a fusion of two ancient gene families: Thioredoxin and ERV1. *Genomics* **54:** 460–468.

Doublie, S. 1997. Preparation of selenomethionyl proteins for phase determination. *Methods Enzymol.* **276:** 523–530.

Dym, O. and Eisenberg, D. 2001. Sequence–structure analysis of FAD-containing proteins. *Protein Sci.* **10:** 1712–1728.

Fetrow, J.S., Siew, N., and Skolnick, J. 1999. Structure-based functional motif identifies a potential disulfide oxidoreductase active site in the serine/threonine protein phosphatase-1 subfamily. *FASEB J.* **13:** 1866–1874.

Francavilla, A., Ove, P., Polimeno, L., Cotzee, M., Makowka, L., Rose, J., Van Thiel, D.H., and Starzl, T.E. 1987. Extraction and partial purification of a hepatic stimulatory substance in rats, mice, and dogs. *Cancer Res.* **47:** 5600–5605.

Gandhi, C.R., Kuddus, R., Subbotin, V.M., Prelich, J., Murase, N., Rao, A.S., Nalesnik, M.A., Watkins, S.C., DeLeo, A., Trucco, M., et al. 1999. A fresh look at augmenter of liver regeneration in rats. *Hepatology* **29:** 1435–1445.

Gross, E., Sevier, C.S., Vala, A., Kaiser, C.A., and Fass, D. 2002. A new FAD-binding fold and intersubunit disulfide shuttle in the thiol oxidase Erv2p. *Nat. Struct. Biol.* **9:** 61–67.

Hagiya, M., Francavilla, A., Polimeno, L., Ihara, I., Sakai, H., Seki, T., Shimonishi, M., Porter, K.A., and Starzl, T.E. 1994. Cloning and sequence analysis of the rat augmenter of liver regeneration (ALR) gene: Expression of biologically active recombinant ALR and demonstration of tissue distribution. *Proc. Natl. Acad. Sci.* **91:** 8142–8146.

Hoober, K.L. and Thorpe, C. 1999. Egg white sulfhydryl oxidase: Kinetic mechanism of the catalysis of disulfide bond formation. *Biochemistry* **38:** 3211–3217.

Hoober, K.L., Sheasley, S.L., Gilbert, H.F., and Thorpe, C. 1999. Sulfhydryl oxidase from egg white. A facile catalyst for disulfide bond formation in proteins and peptides. *J. Biol. Chem.* **274:** 22147–22150.

Jones, T.A. 1991. Improved methods for building protein models in electron density maps and the location of errors in these models. *Acta Crystallogr. A* **47:** 110–119.

Lange, H., Lisowsky, T., Gerber, J., Muhlenhoff, U., Kispal, G., and Lill, R. 2001. An essential function of the mitochondrial sulfhydryl oxidase Erv1p/ALR in the maturation of cytosolic Fe/S proteins. *EMBO Rep.* **2:** 715–720.

Lisowsky, T. 1996. Removal of an intron with unique 3′ branch site creates an amino-terminal protein sequence directing the scERV1 gene product to mitochondria. *Yeast* **12:** 1501–1510.

Lu, C., Li, Y., Zhao, Y., Xing, G., Tang, F., Wang, Q., Sun, Y., Wei, H., Yang, X., Wu, C., et al. 2002. Intracrine hepatopoietin potentiates AP-1 activity through JAB1 independent of MAPK pathway. *FASEB J.* **16:** 90–92.

Mathews, F.S. 1991. New flavoenzymes. *Curr. Opin. Struct. Biol.* **1:** 954–967.

Musard, J.F., Sallot, M., Dulieu, P., Fraichard, A., Ordener, C., Remy-Martin, J.P., Jouvenot, M., and Adami, P. 2001. Identification and expression of a new sulfhydryl oxidase SOx-3 during the cell cycle and the estrus cycle in uterine cells. *Biochem. Biophys. Res. Commun.* **287:** 83–91.

Otwinowski, Z. and Minor, W. 1997. Processing of X-ray diffraction data collected in oscillation mode. *Methods Enzymol.* **276:** 307–326.

Perrakis, A., Morris, R., and Lamzin, V.S. 1999. Automated protein model building combined with iterative structure refinement. *Nat. Struct. Biol.* **6:** 458–463.

Rose, J.P., Wu, C.K., Francavilla, A., Prelich, J.G., Iacobellis, A., Hagiya, M., Rao, A.S., Starzl, T.E., and Wang, B.C. 1997. Crystallization and preliminary crystallographic data for the augmenter of liver regeneration. *Acta Crystallogr. D* **53:** 331–334.

Rose, J.P., Wu, C.K., Dailey, T.A., Dailey, H.A., and Wang, B.C. 1999. P06.04.082 The refined crystal structure of the augmenter of liver regeneration. In *Abstracts of the International Union of Crystallography XVIII Congress and General Assembly.* Glasgow, Scotland.

Senkevich, T.G., White, C.L., Koonin, E.V., and Moss, B. 2000. A viral member of the ERV1/ALR protein family participates in a cytoplasmic pathway of disulfide bond formation. *Proc. Natl. Acad. Sci.* **97:** 12068–12073.

———. 2002. Complete pathway for protein disulfide bond formation encoded by poxviruses. *Proc. Natl. Acad. Sci.* **99:** 6667–6672.

Sevier, C.S., Cuozzo, J.W., Vala, A., Aslund, F., and Kaiser, C.A. 2001. A flavoprotein oxidase defines a new endoplasmic reticulum pathway for biosynthetic disulphide bond formation. *Nat. Cell Biol.* **3:** 874–882.

Terwilliger, T.C. and Berendzen, J. 1999. Automated MAD and MIR structure solution. *Acta Crystallogr. D Biol. Crystallogr.* **55:** 849–861.

White, C.L., Senkevich, T.G., and Moss, B. 2002. Vaccinia virus G4L glutaredoxin is an essential intermediate of a cytoplasmic disulfide bond pathway required for virion assembly. *J. Virol.* **76:** 467–472.